# A New Ratio-Metric pH Probe, "ThiAKS Green" for Live-Cell pH Measurements

Ali AKYOL[1] , Doruk BAYKAL[2], Akın AKDAĞ[2],
Özge ŞENSOY[3], and Çağdaş Devrim SON[1*]

[1]*Middle East Technical University, Department of Biological Sciences, Ankara 06800, Turkey*

[2]*Middle East Technical University, Department of Chemistry, Ankara 06800, Turkey*

[3]*Istanbul Medipol University, School of Engineering and Natural Sciences, İstanbul 34810, Turkey*

[*]Corresponding author: Çağdaş Devrim SON E-mail: cson@metu.edu.tr

**Abstract:** Deviation of the $H^+$ concentration from optimum values within the organelles is closely associated with irregular cellular functions that cause the onset of various diseases. Therefore, determining subcellular pH values in live cells and tissues is valuable for diagnostic purposes. In this study, we report a novel ratiometric fluorescence probe 1H-pyrazole-3-carboxylic acid, 4-(benzo[d]thiazol-2-yl)-3-(2,4-dihydroxy-3-methylphenyl)-1H-pyrazole-5-carboxylicacid4-(2-benz othiazolyl)-5-(2,4-dihydroxy-3-methylphenyl), to which we will refer as ThiAKS Green (Thiazole AKyol shifting green), that is pH sensitive. The results presented here show that the probe can penetrate the cell membrane in less than 30 minutes and does not show any detectable toxicity. The measured color shifts up on pH change are linear and most significant around physiological pH (pKa=7.45), thus making this probe suitable for live-cell imaging and intracellular pH measurements. During the long-incubation periods following the application of the probe and the fluorescent microscopy measurements, it shows stable properties and is easy to detect in live cells. In conclusion, the results suggest that ThiAKS Green can be used to obtain precise information on the $H^+$ distribution at various compartments of the live cells.

**Keywords:** Fluorescent probe; ratiometric sensor; intracellular pH; cell imaging; fluorescent microscopy

Citation: Ali AKYOL, Doruk BAYKAL, Akın AKDAĞ, Özge ŞENSOY, and Çağdaş Devrim SON, "A New Ratio-Metric pH Probe, 'ThiAKS Green' for Live-Cell pH Measurements," *Photonic Sensors*, 2023, 13(1): 230125.

## 1. Introduction

Intracellular pH ($pH_i$) homeostasis is essential for most cellular activities, such as cell volume, vesicle transportation, cellular metabolism, cell membrane polarity, muscle contraction, and cytoskeletal interactions [1–6]. Moreover, the level of intracellular messengers, which has an impact on cell signaling pathways, can also be influenced by $pH_i$ [7, 8]. The $pH_i$ differs in most cellular compartments, which provides unique conditions for maintaining desired reactions [9]. For instance, the lysosome has a slightly acidic environment, which is crucial for the function of this organelle, such as the breakdown and/or recycling of molecules [10]. In contrast, the nucleus and cytoplasm have neutral pH to sustain molecular transfer [11]. The pHs of the Golgi and ER are also known to be around neutral pH, 6.7 and 7.2, respectively [9]. The pH can further fluctuate between different compartments of an

Received: 21 January 2022 / Revised: 17 June 2022

DOI: 10.1007/s13320-022-0666-5
Article type: Regular

organelle due to their functional differences. For example, mitochondria have higher pH in the matrix but near-neutral pH (7 – 7.4) in the intermembrane space [12]. These variations create specific environments for each of these compartments, contributing to their biological functions. Therefore, monitoring the pH changes can enhance our understanding of how physiological and pathological processes proceed [13]. In that respect, the ability to precisely measure the fluctuation in the pH may provide a broadened understanding of certain diseases. Noncharacteristic pH values are often linked to some cancer types [14] and neurodegenerative diseases [15]. The acidic extracellular environment is a typical characteristic observed in many cancer cases and could be related to the invasiveness of malignant cells. Specifically, while the extracellular pH of normal cells is 7.3 – 7.4, it can drop to 6.2 – 6.9 in cancer cells [16].

Intracellular pH differences determine the fate of cellular events and reactions [11]. Detection of abnormal pH values in specific cellular compartments is crucial and may provide an efficient way to understand better the basis of these progressions and dysfunctions [17]. There have been several methods used for pH detection in live cells, including the usage of a pH-sensitive microelectrode that requires a physical insertion of the electrode into each cell or a solution under study. Even though some of these methods provide sensitive pH measurements of the solution by refractive index or surface charge, they can not target a specific cell organelle [18, 19]. Similarly, nuclear magnetic resonance (NMR) measurements can be used to determine the pH differences. All of these methods have been reported to show some difficulty in targeting a specific cell compartment or even a single cell [17]. On the other hand, fluorescence-based ratio-metric pH probes have several advantages over these measurements [13]. These probes can enable visualization of the cells and help differentiate pH within specific cell compartments [20] without harming the cells or disrupting cellular activities caused by methods used for measurement, allowing these probes invaluable for live-cell pH studies [21]. Additionally, the use of ratiometric probes will enable the researcher to carry out systematic error corrections of the measurements [22].

In this study, we have provided a novel, non-toxic ratiometric pH probe that can penetrate through biological membranes, thus enabling the pH measurements in specific compartments of live cells.

## 2. Materials and methods

### 2.1 Reagent

The 1H-Pyrazole-3-carboxylic acid, 4-(2-benzothiazolyl)-5-(2,4-dihydroxy-3-methylphenyl (ThiAKS Green) purchased from InterBioScreen was dissolved in 100% DMSO (dimethyl sulfoxide) at a concentration of 10 mM and stored at –80 ℃ for future use.

### 2.2 Fluorescence and UV-Vis spectrum of the probe at varying pHs

The fluorescence spectrum of the chemical was obtained at 50 μM concentration in 50 mM acetate-acetic acid, 1X PBS (phosphate buffer saline), and 50 mM Glycine-NaOH solutions at pH 4, 7, and 10, respectively. The effect of the incubation period was also tested. Measurements were performed with the Molecular Device Spectramax Id3 microplate reader. The ultraviolet-visible spectroscopy (UV-Vis) spectrum of the compound was obtained in the same buffer solutions at 50 μM concentration in Thermo Scientific Multiscan Go with 1 mL quartz cuvettes with 2 nm bandwidth.

### 2.3 pKa measurement

pKa was calculated by using the fluorescence intensity ratio 450/520 over 360/520 ($I_{450/360}$) in 14 different buffer solutions, pH 4.8, 5.5 (50 mM acetate buffer), 5.8, 6.2, 6.70 (1X PBS), 7.05, 7.20, 7.50, 7.75, 8.05 (50 mM Tris-HCl), 8.25, 8.50, 8.75, 8.95, 9.40 (50 mM Glycine NaOH). Samples were

incubated in these buffers for 1.5 hours at 37 ℃ before fluorescence measurement in Molecular Devices Spectramax id3 plate reader. The excitation and emission bandwidth used were 15 nm and 25 nm, respectively.

### 2.4 Cell culture

HEK 293 (human embryonic kidney) cells were cultured in 90% v/v dulbecco's modified eagle's medium (DMEM) with L-glutamine (Gibco, REF 41966-029), 10% v/v heat-inactivated fetal bovine serum (Biological Industries REF 04-127-1B), and 1% v/v penicillin/ streptomycin solution (Biological Industries REF 03-031-1B). Cells were grown at 37 ℃ in a humidified 95% air and 5% $CO_2$ atmosphere. The cells were routinely sub-cultured twice a week.

### 2.5 MTT toxicity assay

HEK 293 cells were seeded on clear F-bottom plastic 96-well microplates with the density of 20000 cells at 100 µL final volume in the complete medium, then incubated in a cell culture incubator for 20 hours. The test compound was added at 50 µM and 100 µM concentrations and incubated for 4 hours. After that, samples were removed from the incubator, and 10 µL MTT 3-(4,5-dimethylthiazol-2-yl)-2,5-diphenyl-2H- tetrazolium bromide solution was added to each well and incubated for an additional 4 hours. Finally, 100 µL detergent solution [10% sodium dodecyl sulfate (SDS) in 0.01 M HCl] was added to each well to dissolve the formed formazan crystals. The plates were shaken for 5 minutes and then incubated at ambient conditions for 16 hours. Absorbance was measured at 570 nm with Thermo Scientific Varioskan Lux microplate reader.

### 2.6 Ion interference on fluorescence of the probe

The interference on the $I_{450/360}$ ratio of various abundant metal ions and trace elements found in live cells and a redox specie $H_2O_2$ were investigated. For this purpose, each ion and molecule was prepared in 250 mM Tris-HCl buffer at pH 7.35, then 50 µM of ThiAKS Green was added to the solutions. After 1.5 hours of incubation at 37 ℃, fluorescent measurements were carried out by the Molecular Devices Spectramax id3 plate reader.

### 2.7 Fluorescent microscope imaging and intracellular pH measurement

For localization and intracellular pH measurement experiments, 150000 HEK 293 cells were seeded on poly-D-lysine (PDL) coated 35 mm glass-bottom petri dishes. Twenty-four hours later, cells were transfected with NLS-mCh. (nuclear localization signal fused mCherry fluorescent protein) or Golgi-targeted mCh. using Lipofectamine LTX™ transfection reagent. Localization experiments were carried out on NLS-mCh. transfected cells. After 48-hour post-transfection, cell media was aspirated and replaced with either 0.5% (v/v) DMSO or 50 µM of ThiAKS Green containing 1 mL hanks' buffered saline solution (HBSS), then incubated for another 1.5 hours in the cell culture incubator. HBSS buffer was aspirated and replaced with 1X PBS before imaging. Similarly, intracellular pH measurements were carried out in two sets of Golgi-targeted mCh. carrying plasmids transfected HEK 293 cells. After two-day post-transfection, cell media was aspirated and replaced with either 0.5% (v/v) DMSO (for background calculations) or 50 µM of ThiAKS Green containing 1 mL HBSS buffer, then incubated for another 1.5 hours in the cell culture incubator. HBSS buffer was aspirated and replaced with 1X PBS before imaging. All fluorescent microscopy imagings were performed using Leica DMI 4000 Microscopy with a Leica 100X/1.40 HCX APO oil DIC objective. Cells were imaged using DAPI (4′,6-diamidino-2-phenylindole) ($\lambda_{ex}$: 365±20, $\lambda_{em}$: 470±20), EGFP ($\lambda_{ex}$: 485±10, $\lambda_{em}$: 525±25), and mCh ($\lambda_{ex}$: 585±15, $\lambda_{em}$: 630±20) filters. Intensities in DAPI and enhanced green fluorescent protein (EGFP) channels were measured by Image J software for ratiometric calculations.

### 2.8 Computational studies

Computational studies on the fluorophore ThiAKS Green were performed to analyze its electronic structure. All the calculations were performed using the B3LYP/6-311+G(d) basis set as implemented in Gaussian 09 software [23]. Three-dimensional structures were visualized using the Jmol software.

### 2.9 Statistical analysis

All the graphs were plotted in Graphpad Prism version 8.0.1. All experiments were performed in triplicates, and the results were presented as mean ±SEM (standard error of mean). The statistical analyses were carried out in GraphPad Prism using two-way analysis of variance (ANOVA) followed by the Tukey test.

## 3. Results and discussion

### 3.1 Characterization of ThiAKS Green

The chemical structure of ThiAKS Green is shown in Fig. 1.

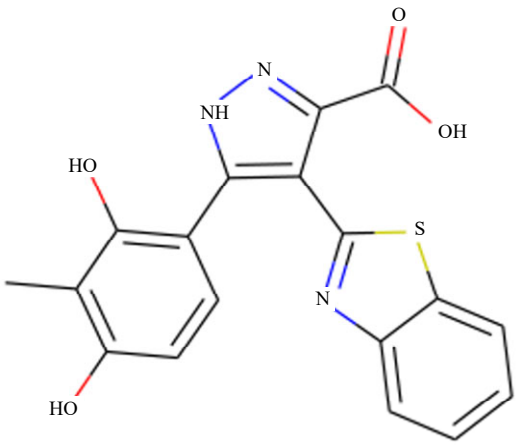


Fig. 1 Chemical structure of ThiAKS Green, 1H-pyrazole-3-carboxylic acid, 4-(benzo[d]thiazol-2-yl)-3-(2,4-dihydroxy-3-methylphenyl)-1H-pyrazole-5-carboxylic acid4-(2-benzothiazolyl)-5-(2,4-dihydroxy-3-methylphenyl). (Taken from ZINC database) CAS Registry number: 384367-09-3.

The UV-Vis absorption spectrum of ThiAKS Green was plotted in various buffer solutions with the following pH values: 4, 7, and 10. The probe showed an absorption maximum at around 230 nm under all conditions tested. Additionally, a second absorption peak was observed around 320 nm at pH 4, whereas this absorption peak was absent in solutions having higher pH values (Fig. 2).

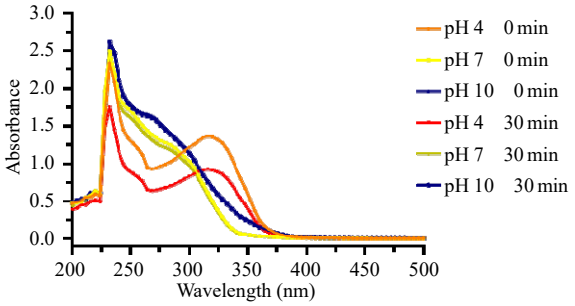


Fig. 2 Absorption spectrum of ThiAKS Green at pH 4.0, 7.0, and 10.0.

The fluorescence properties of the probe were investigated (both excitation and emission spectra were measured) under three different pH values: 4, 7, and 10. The excitation spectrum of the probe ($\lambda_{em}$: 540 nm) showed that a total of three separate excitation peaks existed, and the intensities of these peaks were varied at each pH tested (Fig. 3). In particular, two low-intensity peaks were observed around 275 nm and 365 nm at pH 4, whereas the first excitation peak (275 nm) significantly increased at pH 7. In addition to these two peaks, another excitation peak emerged around 450 nm at pH 10. Notably, 30-minute incubation time improved this excitation peak at pH 10.

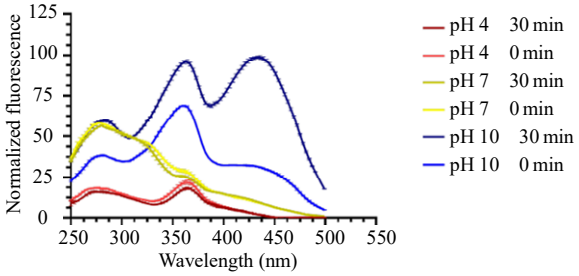


Fig. 3 Excitation spectrum of ThiAKS Green at pH 4, 7, and 10 and the emission wavelength at 540 nm.

The emission spectrum was obtained separately for each excitation peak at 360 nm and 450 nm [Figs. 4(a) and 4(b), respectively]. Relatively low emission intensities were observed at both excitation wavelengths at pH 4. As a result, these findings suggested that the probe had two distinct emission

peaks at 450 nm, and 520 nm.

Observation of improvements in the fluorescent emission intensity at 520 nm upon pH and incubation time variation suggested that high pH values induced a conformational change that resulted in red-shifted fluorescence emission.

Following the observation of a significant intensity increase at 520 nm at high pH, we carried out the pKa calculation using the intensity ratio of $I_{450/360}$ ($\lambda_{ex}$: 450/360 nm; $\lambda_{em}$: 520 nm). The rationale for choosing these wavelengths was to avoid exposure of the cells to intense UV light (275 nm). Moreover, this choice also avoided the necessity of using UV-compatible optics and a UV light source that might be missing on some microscopes. The measured ratio $I_{450/360}$ changed from 0.05 to 0.6 while pH increased from 4.8 to 9.40 (±0.02). Using this ratio, we calculated the pKa value of the probe as 7.45 (Fig. 5). These calculations, with the fact that the pH of most cellular compartments fluctuated around neutral pH levels, provided an advantage to ThiAKS Green compared to the frequently used pH probes in the literature, such as RhB-R12K-FITC [24].

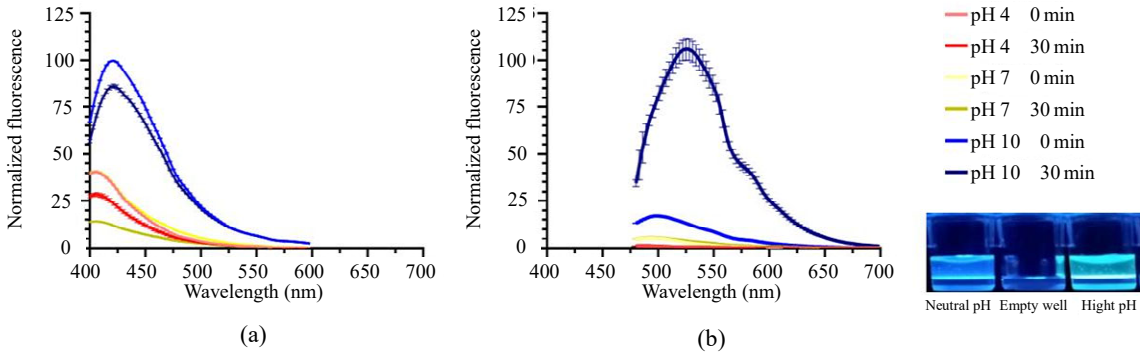


Fig. 4 Emission spectrum of ThiAKS at pH 4.0, 7.0, and 10.0: (a) excitation wavelength at 360 nm and (b) excitation wavelength at 450 nm. Data mean ±SEM experiment performed duplicate.

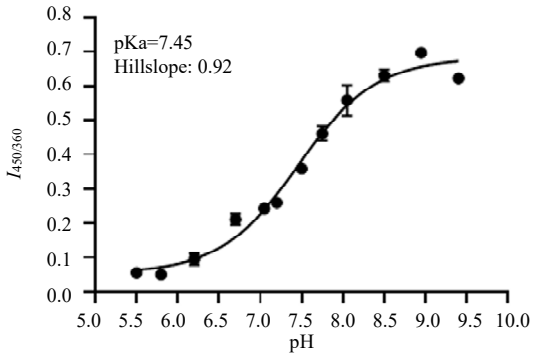


Fig. 5 Plot of pH versus $I_{450/360}$ (emission 520 nm). Data mean ±SEM experiment performed duplicate.

### 3.2 Computational analysis

ThiAKS Green contains a central 1,2-diazole ring, which is responsible for the formation of two tautomer forms, namely, 1H-ThiAKS and 2H-ThiAKS. Computations were carried out using four structures: 1H-ThiAKS, 2H-ThiAKS, as well as their deprotonated carboxylate forms, 1H-ThiAKS-dep and 2H-ThiAKS-dep, respectively. It was found that the protonated form 1H-thiAKS was lower in free energy than the other tautomers, by 5.67 kcal/mol. Interestingly, for the deprotonated form, 2H-thiAKS-dep was lower in energy by 15.27 kcal/mol. This behavior was due to the H-bonding formed between the phenolic hydrogen and the diazole moiety. The calculated free energies of the structures were compared between protonated and deprotonated forms. The highest occupied molecular orbital (HOMO) and lowest unoccupied molecular orbital (LUMO) levels were shown in Table 1, and HUMO-LUMO images were given in Fig. 6. The time dependent density functional theory (TD-DFT) calculations were carried out on the optimized structures to obtain theoretical vertical excitation values. TD-DFT calculations were

performed using the CAM-B3LYP/6-311+G(d) basis set as implemented in Gaussian 09 software. The calculations' accuracy was checked by comparing the experimental UV-Vis absorption spectra to the calculated oscillator strengths. The calculated oscillator strengths of the protonated forms were compared to the absorption data at acidic pH, whereas those of the deprotonated forms were compared to absorption data at basic pH. Both absorption and oscillator strengths were normalized for qualitative comparison (data not shown). The computational results were shown to be in correspondence with corresponding experimental data.

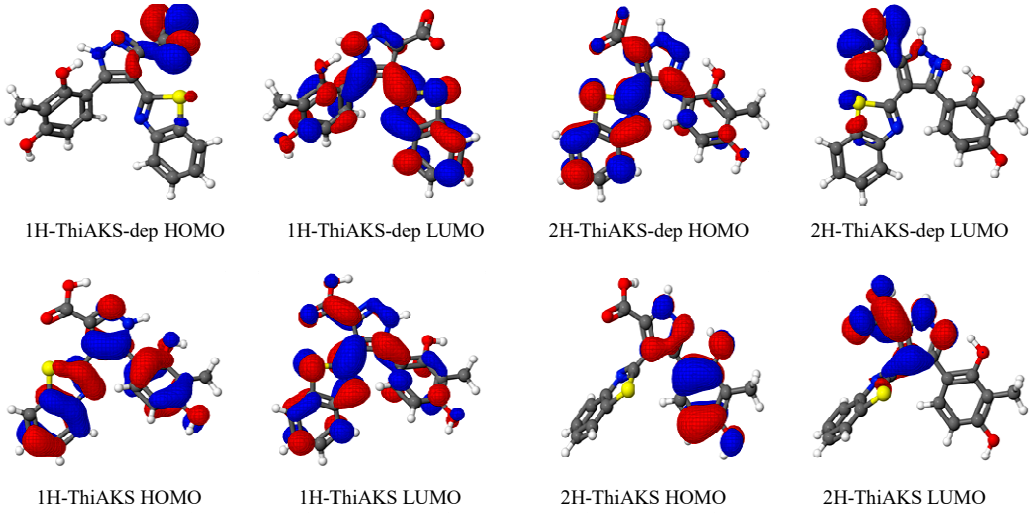


Fig. 6 HOMO-LUMO images of ThiAKS Green.

Table 1 Homo and Lumo levels of the probe.

| | HOMO (eV) | LUMO (eV) | Energy gap (eV) |
|---|---|---|---|
| 1H-ThiAKS | –5.73 | –1.47 | 4.26 |
| 2H-ThiAKS | –5.88 | –2.18 | 3.71 |
| 1H-ThiAKS-dep | –1.58 | 1.52 | 3.11 |
| 2H-ThiAKS-dep | –2.47 | 1.61 | 4.08 |

### 3.3 Toxicity of ThiAKS Green

In order to assess the toxicity of ThiAKS Green, HEK 293 cells were used as a model system. The toxicity of the chemical was tested at two different concentrations (50 μM and 100 μM) with the MTT test (Fig. 7). Since the chemical was dissolved in 100% DMSO, an additional group was used in the test as control which was named "the control veh.". The results showed that, while 1% DMSO caused a ~ 30% decrease in HEK cell viability, this effect almost vanished in the presence of the chemical. This observation indicated the non-toxic character of the chemical. The MTT reagent and ThiAKS Green interaction were also tested in no cell-containing HEK media to ensure the observed results not due to such interactions.

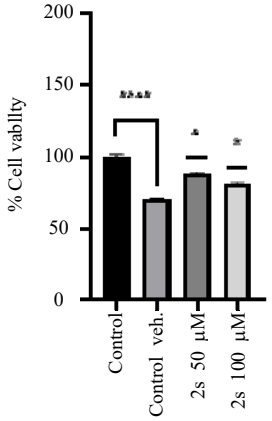


Fig. 7 Toxicity test of the ThiAKS Green at 50 μM and 100 μM concentration. *$p$<0.05, ****$p$<0.000 1 statistically significant differences. Data mean ±SEM experiment performed triplicate replicas.

### 3.4 Interference of abundant ions on ThiAKS Green

The interference of redox species $H_2O_2$ at

100 µM and the most abundant elements in cell $Na^+$, $K^+$, $Ca^{2+}$, and $Mg^{2+}$ were tested at 50 mM, 150 mM, 1 µM, and 1 mM, respectively. The concentrations used were based on the free intracellular concentrations of these elements [25, 26].

Also, we tested some of the trace elements: $Al^{3+}$, $Cu^{2+}$, $Fe^{3+}$, and $Ni^{2+}$ at 1 µM (above intracellular concentrations). Results indicated that $Ni^{2+}$ and $Cu^{2+}$ showed a decreasing effect on the $I_{450/360}$ while other elements had no such interference (data not shown).

We also investigated whether the concentration of the probe altered the $I_{450/360}$ ratio. For this, three different concentrations (25 µM, 50 µM, and 75 µM) of the probe were investigated at pH 7.20 and the $I_{450/360}$ ratio compared to each other (Fig. 8). The results showed that the $I_{450/360}$ ratio was not affected by the concentration of the probe.

### 3.5 Imaging and localization of ThiAKS Green

The intracellular localization of the probe was determined by the fluorescent microscope using HEK cells transfected with the nucleus targeted mCh. carrying plasmid.

After 1.5 hours of exposure to 50 µM of the probe or 0.5% (v/v) DMSO, samples were imaged in bright-field, DAPI, EGFP, and mCh. channels (Fig. 9). The probe could be detected in the cytoplasm and emitted strong fluorescence around the cell membrane.

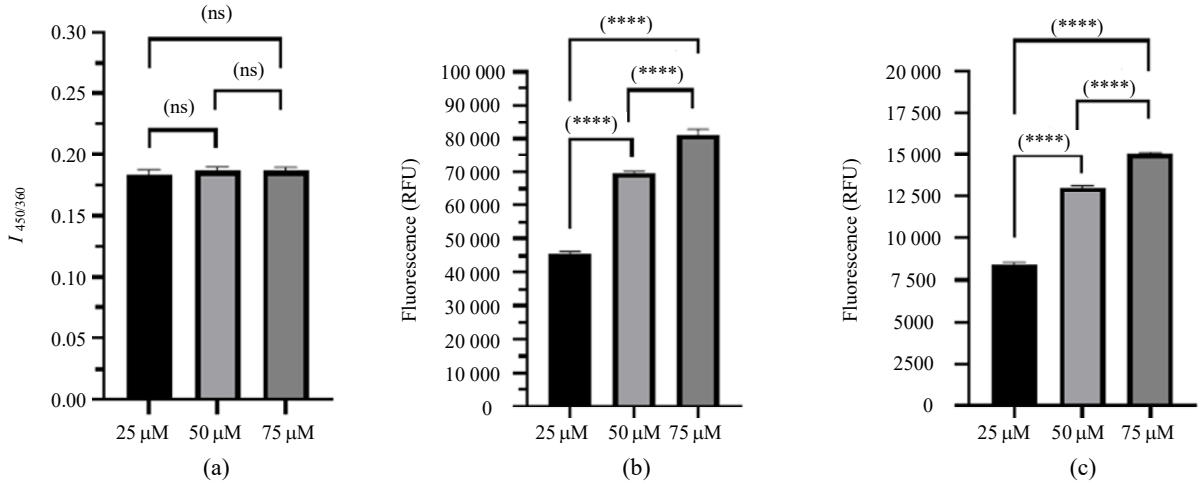


Fig. 8 Concentration effect on ratio $I_{450/360}$ at pH:7.20: (a) ratio $I_{450/360}$ (emission 520 nm), (b) intensity in 360/520, and (c) intensity in 450/520. ****$p$<0.0001 statistically significant differences. ns: no significant differences. Data mean ±SEM experiment performed triplicate.

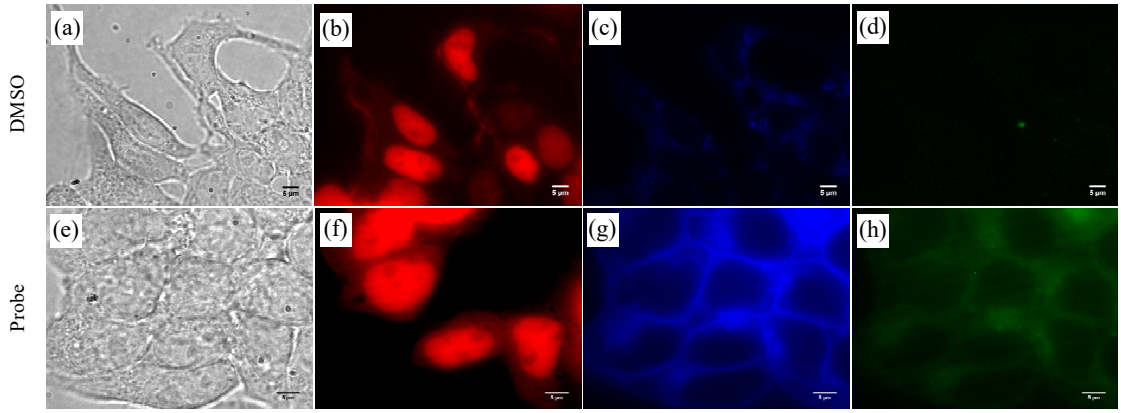


Fig. 9 Fluorescent microscope images of NLS-mCh. expressing HEK 293 cells treated with 0.5% DMSO [(a)–(d)] or 50 µM ThiAKS Green [(e)–(h)] for 1.5 hours: (a) bright-field image, (b) mCh. channel, (c) DAPI Channel, (d) EGFP channel, (e) bright-field image, (f) mCh. channel, (g) DAPI channel, and (h) EGFP channel. (Magnification 100X, scale bars are 5 µm).

### 3.6 Intracellular pH measurement of HEK 293 cells

To demonstrate that ThiAKS Green was suitable for measuring intracellular pH, we used HEK 293 cells as a model system, and the Golgi organelle was chosen for the pH measurement as a proof of concept measurement. First, we plotted a calibration curve for $I_{450/360}$, which indicated a 10-fold increase between pH 5.9 and 8.0 (Fig. 10).

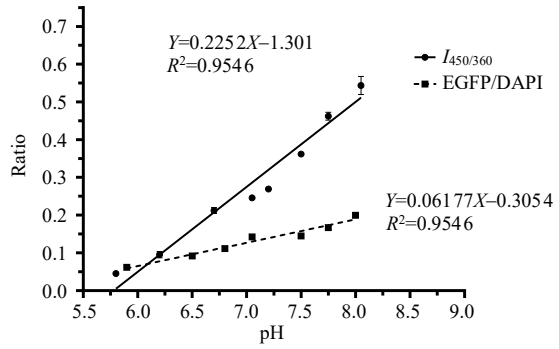


Fig. 10 Calibration curve EGFP/DAPI and $I_{450/360}$.

As a proof of concept, we chose to demonstrate the pH measurement of the Golgi by using the EGFP/DAPI ratio. Considering the microscopes might have different light sources and filters for each channel, we measured the intensity of the light coming out of the objective lens (both LUX and photon count) with the help of a luminometer. In order to make each channel's intensity comparable, the excitation power of each line was adjusted accordingly. Following these adjustments, we measured the pH of intracellular organelles such as the Golgi (taking advantage of a Golgi-targeted mCh. for determining the region of interest around Golgi). Only DMSO treated sample (figures not shown) was used for background calculations. The ratio of EGFP/DAPI was calculated by ImageJ software and extrapolated with the equation obtained from the calibration curve (Fig. 10). In agreement with the literature, our calculated results showed that the pH of the Golgi was 6.75. Meanwhile, the pH of the cell membrane was calculated as 6.38. (Fig. 11).

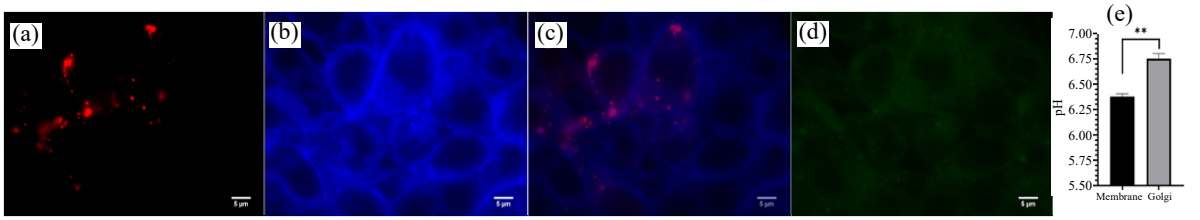


Fig. 11 Fluorescent microscope images of HEK cells transfected with Golgi targeted mCh. and treated with 50 μM ThiAKS Green: (a) mCh. channel, (b) DAPI channel, (c) overlay of (a) and (b), (d) image from EGFP channel, and (e) calculated pH from ratio EGFP/DAPI intensities of membrane and Golgi (Magnification 100X, scale bars are 5 μm).

## 4. Conclusions

The results presented in this study indicated that the new small organic fluorescent pH probe "ThiAKS Green" was suitable for intracellular pH measurements. This new probe had no cell toxicity at 50 μM and 100 μM concentrations tested during this study and showed adequate cell-penetrating properties for microscopy imaging. Moreover, the calculated pKa value (7.45) suggested that the probe was ideal for $pH_i$ measurement. Although it was observed that the ThiAKS Green was located throughout the live cells, it was readily detectable around the cell membrane. This allowed direct measurements of the membrane pH without the necessity of specific probe targeting. These observations suggested that the probe could be convenient in cancer-related studies for measuring membrane pH fluctuations. The availability of at least two different ratios that could be used to calculate $pH_i$ made this probe suitable for various instruments that could have limited excitation and emission capabilities. Although the EGFP/DAPI ratio was less sensitive than the $I_{450/360}$ ratio, it was

sufficient to distinguish pH 6.75 from pH 6.38 under our experimental conditions using a standard fluorescent microscope. Nevertheless, in need of a more sensitive measurement, $I_{450/360}$ ratio can be used.

## Acknowledgment

We thank SON Lab, undergraduate "special project student" Tolgahan Suat Sezen, for his help. Golgi and nucleus markers were provided by former SON Lab member Hüseyin Evci.



## References

[1] M. Ritter, E. Wöll, D. Häussinger, and F. Lang, "Effects of bradykinin on cell volume and intracellular pH in NIH 3T3 fibroblasts expressing the ras oncogene," *FEBS Letters*, 1992, 307(3): 367–370.

[2] T. M. Nosek, K. Y. Fender, and R. E. Godt, "It is diprotonated inorganic phosphate that depresses force in skinned skeletal muscle fibers," *Science*, 1987, 236(4798): 191–193.

[3] D. Joseph, "Alveolar Epithelial Ion and Fluid Transport Polarity of alveolar epithelial cell acid-base permeability," *American Journal of Physiology-Lung Cellular and Molecular Physiology*, 2002, 282(4), L675–L683.

[4] W. Hao, Z. Luo, L. Zheng, K. Prasad, and E. M. Lafer, "AP180 and AP-2 interact directly in a complex that cooperatively assembles clathrin," *Journal of Biological Chemistry*, 1999, 274(32): 22785–22794.

[5] B. T. Edmonds, J. Murray, and J. Condeelis, "pH regulation of the F-actin binding properties of dictyostelium elongation factor 1α," *Journal of Biological Chemistry*, 1995, 270(25): 15222–15230.

[6] W. B. Busa and R. Nuccitelli, "Metabolic regulation via intracellular pH," *American Journal of Physiology, Regulatory, Integrative and Comparative Physiology*, 1984, 15(4): 409–438.

[7] C. J. Brokaw, "Regulation of sperm flagellar motility by calcium and cAMP-dependent phosphorylation," *Journal of Cellullar Biochemistry*, 1987, 35(3): 175–184.

[8] T. Speake and A. C. Elliott, "Modulation of calcium signals by intracellular pH in isolated rat pancreatic acinar cells," *Journal of Physiology*, 1998, 506(2): 415–430.

[9] J. R. Casey, S. Grinstein, and J. Orlowski, "Sensors and regulators of intracellular pH," *Nature Reviews Molecular Cell Biology*, 2010, 11(1): 50–61.

[10] H. Xu and D. Ren, "Lysosomal physiology," *Annual Review of Physiology*, 2015, 77: 57.

[11] P. C. Caldwell, "Intracellular pH," *International Review of Cytology*, New York: Academic Press, 1956.

[12] H. Xiao, Y. Dong, J. Zhou, Z. Zhou, X. Wu, R. Wang, *et al.*, "Monitoring mitochondrial pH with a hemicyanine-based ratiometric fluorescent probe," *Analyst*, 2019, 144(10): 3422–3427.

[13] M. C. Xia, L. Cai, S. Zhang, and X. Zhang, "A cell-penetrating ratiometric probe for simultaneous measurement of lysosomal and cytosolic pH change," *Talanta*, 2018, 178: 355–361.

[14] P. Zhang, J. Meng, Y. Li, Z. Wang, and Y. Hou, "pH-sensitive ratiometric fluorescent probe for evaluation of tumor treatments," *Materials (Basel)*, 2019, 12(10): 1632.

[15] P. P. Y. Lie and R. A. Nixon, "Lysosome trafficking and signaling in health and neurodegenerative diseases," *Neurobiology of Disease*, 2019, 122: 94–105.

[16] A. C. Alves, D. Ribeiro, C. Nunes, and S. Reis, "Biophysics in cancer: the relevance of drug-membrane interaction studies," *Biochimica Et Biophysica Acta (BBA)-Biomembranes*, 2016, 1858(9): 2231–2244.

[17] T. Bagar, K. Altenbach, N. D. Read, and M. Benčina, "Live-cell imaging and measurement of intracellular pH in filamentous fungi using a genetically encoded ratiometric probe," *Eukaryotic Cell*, 2009, 8(5): 703.

[18] K. Watanabe, Y. Kishi, S. Hachuda, T. Watanabe, M. Sakakemoto, Y. Nishijima, *et al.*, "Simultaneous detection of refractive index and surface charges in nanolaser biosensors simultaneous detection of refractive index and surface charges in nanolaser biosensors," *Applied Physics Letters*, 2015, 106(2): 021106.

[19] D. Li, H. Zhang, Z. Li, L. Zhou, M. Zhang, X. Pu, *et al.*, "High sensitivity pH sensing by using a ring resonator laser integrated into a microfluidic chip," *Optics Express*, 2022, 30(3): 4106–4116.

[20] Y. Zhang, Y. Zhao, Y. Wu, B. Zhao, L. Wang, and B. Song, "Hemicyanine based naked-eye ratiometric fluorescent probe for monitoring lysosomal pH and its application," *Spectrochimica Acta – Part A: Molecular and Biomolecular Spectroscroscopy*, 2020, 227: 117767.

[21] Y. Zhang, S. Tang, L. Sansalone, J. D. Baker, and F. M. Raymo, "A photoswitchable fluorophore for the real-time monitoring of dynamic events in living organisms," *Chemistry-A European Journal*, 2016, 22(42): 15027–15034.

[22] V. I. Martynov, A. A. Pakhomov, N. V. Popova, I. E. Deyev, and A. G. Petrenko, "Synthetic fluorophores for visualizing biomolecules in living systems," *Acta Naturae*, 2016, 8(4): 33–46.

[23] M. J. Frish, G. W. Trucks, H. B. Schlegel, G. E. Scuseria, M. A. Robb, J. R. Cheeseman, *et al.*, "Gaussian 09, revision A.02." *Gaussian Inc, Wallingford CT*, 2009.

[24] M. C. Xia, L. Cai, S. Zhang, and X. Zhang, "A cell-penetrating ratiometric probe for simultaneous measurement of lysosomal and cytosolic pH change," *Talanta*, 2018, 178: 355–361.

[25] A. M. P. Romani, "Intracellular magnesium homeostasis," *Archives of Biochemistry and Biophysic*, 2011, 512(1): 13–58.

[26] S. Niederer, "Regulation of ion gradients across myocardial ischemic border zones: a biophysical modelling analysis," *PLoS One*, 2013, 8(4): e60323.